Hindawi
Journal of Robotics
Volume 2023, Article ID 1186719, 12 pages
https://doi.org/10.1155/2023/1186719

Research Article

Design of a Novel NNs Learning Tracking Controller for Robotic Manipulator with Joints Flexibility

Pengxiao Jia

College of Science, Beijing Forestry University, Beijing 100083, China

Correspondence should be addressed to Pengxiao Jia; jiapengxiao@126.com

Received 23 April 2023; Revised 25 June 2023; Accepted 6 July 2023; Published 9 August 2023

Academic Editor: Weitian Wang

The precise tracking control problem for the robotic manipulator with flexible joints, subjected to system uncertainties and external disturbances, is addressed. A novel control scheme is presented that does not use link velocity measurements and high-order derivatives of the link states. The control scheme employs neural networks-based observers to estimate both motor velocity and link velocity. By using the virtually applied torque, the link controller is designed based on rigid link dynamics, and the motor controller is designed using the dynamic surface control technique. The proposed control scheme can guarantee that all the signals in the closed-loop system are semiglobally uniformly ultimately bounded, and the tracking error eventually converges to a small neighborhood around zero. The simulation results confirm our theoretical analysis, and a comparison study demonstrates the advantages of the proposed control scheme compared to the standard DSC method.

1. Introduction

In recent years, robots have become standard collaborators not only in factories, hospitals, and offices but also in people's homes, where they can play an important role in situations where a human cannot complete a task alone or needs the help of another person [1]. Flexible joints are extensively used in collaborative robots because, when a robotic manipulator with flexible joints (RMFJ) encounters obstacles during operation, the contact force between the RMFJ and obstacles may be relatively slight, allowing the RMFJ to stop immediately [2]. However, the introduction of joint flexibility in the robot model considerably complicates the equations of motion. The order of the related dynamics becomes twice that of rigid robots, and the number of degrees of freedom is larger than the number of control inputs. Therefore, achieving precise trajectory tracking control for RMFJ is difficult. Moreover, severe nonlinearities, coupling stemming from joint flexibility, structured and unstructured dynamical uncertainties, physical limitations, etc., are typical challenges that need to be addressed [3, 4].

To address the above problems, researchers have proposed a variety of control strategies for the tracking control of RMFJ including PD control [5], singular perturbation control [6, 7], backstepping control [8–10], adaptive control [11, 12], variable structure control [13, 14], intelligent control [15–18], and observer-based control [19, 20]. In particular, the backstepping technique is known as one of the popular techniques for controlling RMFJ. However, the backstepping technique has a drawback called the "explosion of complexity," which is caused by the repeated differentiations of virtual controllers. Swaroop et al. [21] proposed a dynamic surface control (DSC) technique to solve this problem by introducing a first-order filter at each step of the traditional backstepping design. Many other useful research results have been reported for the control problems of various nonlinear real systems [22–24]. However, these proposed DSC schemes do not consider the errors caused by the introduction of filters, which may limit the performance of the system. As an alternative to DSC, command filtered-based control, proposed by Farrell et al. [25], can avoid the problem of the "explosion of complexity." An error compensation mechanism can be constructed to compensate for filter errors and achieve better system tracking performance. The command-filtered technique has been successfully applied to

RMFJ, and the desired control goals have been achieved by Ling et al. [26].

We all know that RMFJ inevitably suffers from nonlinear uncertainties due to unknown loads, inevitable friction, and electric motor aging. When these uncertainties are not addressed, the performance of the system will be seriously affected. With the development of intelligent control, approximating uncertain terms through neural networks (NNs) [16] and fuzzy logic systems (FLSs) [27] has become an effective control method for RMFJ. Shi et al. [18] propose a pattern-based control scheme for constrained flexible joint manipulators using the approximation and learning capabilities of NNs. The output constraint problem is handled through system transformation. Ling et al. [28] propose an adaptive fuzzy DSC scheme for single-link flexible-joint robotic systems with input saturation. The problem of input saturation is addressed by choosing a smooth function for approximation, and FLSs are used to approximate unknown continuous functions.

In addition to tracking issues, addressing the practical limitations of nonlinear systems during operation is very significant in applications. From a practical viewpoint, as pointed out in [29], in practical robotic systems, all the generalized coordinates can be precisely measured by the encoder for each joint. However, velocity measurements obtained through tachometers are easily perturbed by noise. Moreover, in today's robotic applications, velocity sensors are frequently omitted due to considerable reductions in production costs, size, and weight of servo drives. Therefore, in order to align with economic and/or practical constraints, designing control strategies for robot dynamics based on nonlinear observers is of interest.

It is worth noting that, in order to achieve good control performance when designing the controller for RMFJ, it is necessary to consider two aspects. On one hand, the characteristics of the dynamic model need to be taken into account, such as high-order dynamics, uncertainty, nonlinearity, etc. On the other hand, practical limitations of the actual control system for RMFJ must also be considered. These limitations include immeasurable states, signal delays, unmodeled dynamics, periodic disturbances, and various constraints arising from physical limitations or security issues, especially during repetitive movements [9].

In this paper, we address the precise tracking control problem for RMFJ subjected to system uncertainties, external disturbances, and without link velocity. It is worth noting that there have been many excellent research results on this issue. Due to the introduction of flexible joints, the order of the RMFJ dynamics becomes twice that of rigid robots, and the RMFJ dynamics can be divided into robot dynamics and actuator dynamics. To solve the tracking control of flexible-joint manipulators, the concept of "virtually applied torque" is introduced [29]. The elastic force in robot dynamics is treated as a virtually applied torque, allowing the robot dynamics to be viewed as a conventional rigid robotic system. Inspired by this work, in this paper, we present a novel control scheme that does not require link velocity measurements and high-order derivatives of the link states. The proposed control scheme employs nonlinear observers to estimate both the motor velocity and link velocity. By using the concept of "virtually applied torque," the link controller is designed based on rigid link dynamics, and the motor controller is designed using the DSC technique. NNs are used to approximate the uncertainties and disturbances of robot dynamics and motor dynamics. In comparison with the standard DSC method, the main contributions of this paper can be summarized in two parts as follows:

(1) A novel NNs-based tracking control scheme for RMFJ, subjected to system uncertainties and external disturbances, is proposed. The control scheme consists of a rigid link controller and a motor controller. DSC only acts on motor dynamics, reducing the error accumulation caused by introducing first-order filters.

(2) The proposed control scheme does not require link velocity measurements and high-order derivatives of the link states, such as acceleration and jerk. This makes it more suitable for practical applications.

It is shown that the proposed control scheme can guarantee the semiglobal uniform ultimate boundedness of all signals in the closed-loop system. A comparison is conducted to further demonstrate the main contribution of our proposed control scheme.

The rest of this paper is organized as follows: Section 2 presents the problem formulation and preliminaries, Section 3 states the control problems and the proposed solutions. Additionally, simulation results are shown in Section 4 to verify the effectiveness and potential of the proposed control scheme. Finally, Section 5 concludes with a summary of the obtained results.

2. Model Description and Problem Formulation

In general, the nominal dynamic models of an n-link RMFJ consist of robot dynamics and motor dynamics, which can be described using the following forms [26].

$$D(q_l)\,\ddot{q}_l + C(q_l, \dot{q}_l)\dot{q}_l + G(q_l) + k(q_l - q_r) = 0, \tag{1}$$

$$J\,\ddot{q}_r - k(q_l - q_r) = \tau, \tag{2}$$

where $q_l \in R^n$ denotes the link position, $D(q_l) \in R^{n\times n}$ is the inertia matrix. $C(q_l, \dot{q}_l) \in R^{n\times n}$ denotes the coriolis and centripetal forces, $G(q_l) \in R^n$ is the gravity vector, $q_r \in R^n$ denotes the motor position, k represents the joint flexibility, and $J \in R^{n\times n}$ is the motor inertia. The control vector $\tau \in R^n$ is used as the torque input at each motor.

Property 1. The link inertia matrix $D(q_l)$ is symmetric, positive definite. Both $D(q_l)$ and $D^{-1}(q_l)$ are uniformly bounded as follows: $\|D(q_l)\|_2 \le M_D$ and $\|D(q_l)^{-1}\|_2 \le M_{ID}$. Since k is a constant matrix, $\|D(q_l)^{-1}k\|_2 \le M_{Dk}$, where M_D, M_{ID} and M_{Dk} are positive constants.

The nominal values $D(q_l)$, $C(q_l, \dot{q}_l)$, $G(q_l)$, k, and J may be different from the actual values $\overline{D}(q_l)$, $\overline{C}(q_l, \dot{q}_l)$, $\overline{G}(q_l)$, $\overline{k}$, and $\overline{J}$, respectively, due to model uncertainties and external disturbances. If the robot and the motor are further perturbed by external disturbances, the actual dynamics of the nominal RMFJ (1) and (2) can be expressed as follows:

$$\overline{D}(q_l)\,\ddot{q}_l + \overline{C}(q_l, \dot{q}_l)\dot{q}_l + \overline{G}(q_l) + \overline{k}(q_l - q_r) = 0, \tag{3}$$

$$\overline{J}\,\ddot{q}_r - \overline{k}(q_l - q_r) = \tau. \tag{4}$$

Assumption 1. Suppose that, for a given RMFJ, only the nominal values $D(q_l)$, $C(q_l, \dot{q}_l)$, $G(q_l)$, k, and J are known, but the actual values $\overline{D}(q_l)$, $\overline{C}(q_l, \dot{q}_l)$, $\overline{G}(q_l)$, $\overline{k}$, and $\overline{J}$, including the model uncertainties and external disturbances, are unknown.

Assumption 2. The system states q_l and q_r are both available for feedback.

Property 2. $C(q_l, \dot{q}_l)\dot{q}_l$ is bounded as follows: $\|C(q_l, \dot{q}_l)\dot{q}_l\|_2 \le M_C$, where M_C is a positive constant.

Property 3. The matrix $\dot{D}(q_l) - 2C(q_l, \dot{q}_l)$ is skew-symmetric.

The actual dynamics of RMFJ (3) and (4) can be rewritten in the following formulation using the nominal model:

$$D(q_l)\,\ddot{q}_l + C(q_l, \dot{q}_l)\dot{q}_l + G(q_l) + k(q_l - q_r) + E_l = 0, \tag{5}$$

$$J\,\ddot{q}_r - k(q_l - q_r) + E_r = \tau, \tag{6}$$

where $E_l(q_l, \dot{q}_l, q_r) = D(q_l)\overline{D}^{-1}(q_l)\left[\overline{C}(q_l, \dot{q}_l)\dot{q}_l + \overline{G}(q_l) + \overline{k}(q_l - q_r) + \tau_{dl}\right] - \left[C(q_l, \dot{q}_l)\dot{q}_l + G(q_l) + k(q_l - q_r)\right]$ and $E_r(q_l, q_r, \dot{q}_r, \tau) = J\overline{J}^{-1}\left[-\tau - \overline{k}(q_l - q_r) + \tau_{dr}\right] + \left[\tau + k(q_l - q_r)\right]$ denote the uncertainties of robot dynamics and motor dynamics of RMFJ, respectively, τ_{dl} and τ_{dr} are the external disturbances.

As a preliminary to the control design, if we define the state space variables as $x_1 = q_l$, $x_2 = \dot{q}_l$, $x_3 = q_r$, and $x_4 = \dot{q}_r$, the RMFJ with uncertainty terms (5) and (6) is described as follows:

$$\dot{x}_1 = x_2, \tag{7}$$

$$D(x_1)\dot{x}_2 + C(x_1, x_2)x_2 + G(x_1) + E_l = k(x_3 - x_1), \tag{8}$$

$$\dot{x}_3 = x_4, \tag{9}$$

$$J\dot{x}_4 - k(x_1 - x_3) + E_r = \tau. \tag{10}$$

For Assumption 1, the uncertainty terms E_l and E_r cannot be directly evaluated. In this paper, NNs will be employed to observe the uncertainty terms. It has been previously recognized that any continuous function can be uniformly approximated by a linear combination of Gaussians. Hence, the following expressions exist as follows:

$$E_l(x_l) = W_l^T\psi(x_l) + \varpi_l, \tag{11}$$

$$E_r(x_r) = W_r^T\psi(x_r) + \varpi_r, \tag{12}$$

where $x_l = (x_1, x_2, x_3)$ and $x_r = (x_1, x_2, x_3, \tau)$ are the input vectors, W' and W_r denote the optimal weights in the approximate to ensure that the approximation error, and ϖ_l and ϖ_r are as small as possible. ϖ_l and ϖ_r are bounded approximation errors.

Remark 1. In recent years, NNs have undergone rapid development, and many advanced NN models have been proposed. This paper focuses on designing a new control scheme using the concept of "virtually applied torque." It mainly demonstrates the development of controllers and NN tuning laws within a framework. Therefore, a simple RBF (radial basis function) NN model is chosen to approximate the unknown nonlinear system functions. In future work, more advanced NN models will be explored to investigate new control algorithms.

Definition 1. (SGUUB) [30]: The solution $x(t)$ of the system is semiglobally uniformly ultimately bound (SGUUB) if for any compact set Ω and all $x(t_0) \in \Omega$, there exists an $\mu > 0$ and $T(\mu, x(t_0))$ such that $\|x(t)\| \le \mu$ for all $t > t_0 + T$.

In this paper, the trajectory tracking control problem for RMFJ is investigated. The main objective of this research is to ensure that the RMFJ tracking errors are semiglobally uniformly ultimately bounded (SGUUB), even in the presence of system uncertainties, external disturbances, and the absence of link velocity signals.

3. Control Design

3.1. Control Scheme. In this section, we first focus on the rigid part (8) of RMFJ. By considering the elastic force $k(x_3 - x_1)$ as a virtually applied torque, this part can be treated as a conventional rigid robotic system. It is important to note that, compared to flexible robotic systems, there is a wealth of research available on the design of controllers for rigid robotic systems. Under Assumption 2, where the system state x_1 is available for feedback, the reference trajectory of the motor x_{3d} can be determined using the rigid control law for RMFJ tracking. Subsequently, the motor controller can be designed to track this trajectory.

Therefore, in this paper, a NNs-based tracking control scheme is developed for RMFJ, considering system uncertainties, external disturbances, and the absence of link velocity signals, by utilizing the concept of "virtually applied torque." The schematic diagram of the proposed control scheme is shown in Figure 1. The control scheme employs a nonlinear observer to estimate both the motor velocity and link velocity. The link controller is designed based on rigid link dynamics, while the motor controller is designed using

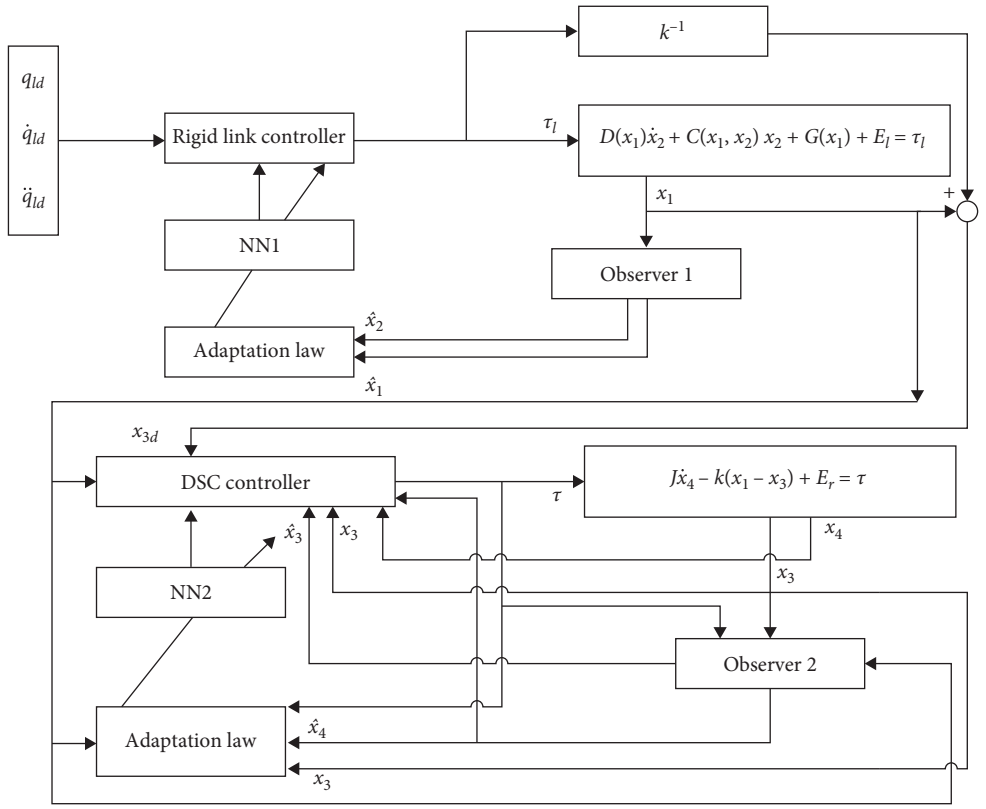

FIGURE 1: Block diagram of the control scheme.

the DSC technique. Additionally, the NNs are utilized to approximate uncertainties and disturbances of robot dynamics and motor dynamics.

Remark 2. A similar control scheme is used in literature [29], but it adopts the backstepping method. To avoid the drawback of "explosion of complexity," we utilize the DSC technique to design the motor controller.

Remark 3. A practical and effective controller for RMFJ is designed in literature [2] based on motor state feedback and the DSC technique. However, the use of too many first-order filters can lead to accumulated errors in the system's boundary layer and reduce control accuracy. In this paper, by employing the concept of "virtually applied torque," we only utilize the DSC technique to design the controller for motor dynamics. This approach helps to reduce the error accumulation caused by introducing first-order filters.

Since the link velocity is not available, nonlinear observers are used to estimate both the motor velocity and link velocity. In the development of the observers and the controllers, all quantities with "^" represent estimated quantities. In addition, quantities with "~" represent estimation error vectors. The position estimation error is given by $\tilde{x} = x - \widehat{x}$.

The estimates $\widehat{x}_1$ and $\widehat{x}_2$ of the system state are defined as follows:

$$\begin{aligned} \widehat{x}_1 &= \widehat{z}_1 \\ \widehat{x}_2 &= \widehat{z}_2 + \kappa_l \widetilde{x}_1, \end{aligned} \tag{13}$$

where $\tilde{x}_1$ is the link position estimation error, and κ_l is a positive constant.

The designed observer takes the form of

$$\begin{aligned} \dot{\widehat{z}}_1 &= \widehat{x}_2 + H_1 \tilde{x}_1 \\ D(x_1)\dot{\widehat{z}}_2 + C(x_1, \widehat{x}_2)\widehat{x}_2 + G(x_1) + \widehat{E}_l(\widehat{x}_l) &= k(x_3 - x_1) + H_2 \tilde{x}_1, \end{aligned} \tag{14}$$

where $\widehat{x}_l = (x_1, \widehat{x}_2, x_3)$, H_1 and H_2 are observer gain matrices. $\widehat{E}_l(\widehat{x}_l) = \widehat{W}_l^T \psi(\widehat{x}_l)$ and $\widehat{W}$ represent the current values of the NNs weights as provided by the adaptive law.

Therefore, the link observer can be rewritten in terms of $\widehat{x}_1$ and $\widehat{x}_2$ as follows:

$$\begin{aligned} \dot{\widehat{x}}_1 &= \widehat{x}_2 + H_1 \widetilde{x}_1 \\ D(x_1)\left(\dot{\widehat{x}}_2 - \kappa_l \dot{\widetilde{x}}_1\right) + C(x_1, \widehat{x}_2)\widehat{x}_2 + G(x_1) + \widehat{W}_l^T \psi(\widehat{x}_l) &= k(x_3 - x_1) + H_2 \widetilde{x}_1. \end{aligned} \tag{15}$$

Considering $\dot{\tilde{x}}_1 = \dot{x}_1 - \dot{\widehat{x}}_1 = x_2 - \widehat{x}_2 - H_1\tilde{x}_1 = \tilde{x}_2 - H_1\tilde{x}_1$, the link observer can be rewritten as follows:

$$\begin{aligned} \dot{\widehat{x}}_1 &= \widehat{x}_2 + H_1\widetilde{x}_1 \\ D(x_1)\dot{\widehat{x}}_2 + C(x_1,\widehat{x}_2)\widehat{x}_2 + G(x_1) + \widehat{W}_l^T\psi(\widehat{x}_l) &= k(x_3 - x_1) + D(x_1)\kappa_l\widetilde{x}_2 + (H_2 - D(x_1)\kappa_l H_1)\widetilde{x}_1. \end{aligned} \tag{16}$$

The error dynamics of the link observer is obtained from (16) and (8) as follows:

$$\begin{aligned} \dot{\widetilde{x}}_1 &= \widetilde{x}_2 - H_1\widetilde{x}_1 \\ D(x_1)\dot{\widetilde{x}}_2 - C(x_1,\widehat{x}_2)\widehat{x}_2 + C(x_1,x_2)x_2 + \widetilde{W}_l^T\psi(\widehat{x}_l) + w_l &= -D(x_1)\kappa_l\widetilde{x}_2 - (H_2 - D(x_1)\kappa_l H_1)\widetilde{x}_1)\kappa_l H_1)\widetilde{x}_1, \end{aligned} \tag{17}$$

where $\tilde{W}_l T = W_l^T - \widehat{W}_l^T$, $w_l = W_l^T[\psi(x_l) - \psi(\widehat{x}_l)] + \varpi_l$.

Similar to the design of the link observer, the estimates $\widehat{x}_3$ and $\widehat{x}_4$ are defined as follows:

$$\begin{aligned} \widehat{x}_3 &= \widehat{z}_3 \\ \widehat{x}_4 &= \widehat{z}_4 + \kappa_r\widetilde{x}_3, \end{aligned} \tag{18}$$

where $\tilde{x}_3$ is the motor position estimation error, and κ_r is a positive constant.

The designed motor observer takes the form of:

$$\begin{aligned} \dot{\widehat{z}}_3 &= \widehat{x}_4 + H_3\widetilde{x}_3 \\ J\dot{\widehat{z}}_4 - k(x_1 - x_3) + \widehat{W}_r^T\psi(\widehat{x}_r) &= \tau + H_4\widetilde{x}_3, \end{aligned} \tag{19}$$

where $\widehat{x}_r = (x_1, x_3, \widehat{x}_4, \tau)$, H_3 and H_4 are observer gain matrix. $\widehat{E}_r(\widehat{x}_r) = \widehat{W}_r^T\psi(\widehat{x}_r)$, $\widehat{W}$ represents the current values of the NNs weights as provided by the adaptive law.

Therefore, the motor observer can be rewritten as follows:

$$\begin{aligned} \dot{\widehat{x}}_3 &= \widehat{x}_4 + H_3\widetilde{x}_3 \\ J\left(\dot{\widehat{x}}_4 - \kappa_r\dot{\widetilde{x}}_3\right) - k(x_1 - x_3) + \widehat{W}_r^T\psi(\widehat{x}_r) &= \tau + H_4\widetilde{x}_3. \end{aligned} \tag{20}$$

Considering $\dot{\tilde{x}}_3 = \dot{x}_3 - \dot{\widehat{x}}_3 = x_4 - \widehat{x}_4 - H_3\tilde{x}_3 = \tilde{x}_4 - H_3\tilde{x}_3$, the motor observer can be rewritten as follows:

$$\begin{aligned} \dot{\widehat{x}}_3 &= \widehat{x}_4 + H_3\widetilde{x}_3 \\ J\dot{\widehat{x}}_4 - k(x_1 - x_3) + \widehat{W}_r^T\psi(\widehat{x}_r) &= \tau + H_4\widetilde{x}_3 + J\kappa_r(\widetilde{x}_4 - H_3\widetilde{x}_3). \end{aligned} \tag{21}$$

The error dynamics of the motor observer is obtained from (21) and (10).

$$\begin{aligned} \dot{\widetilde{x}}_3 &= \widetilde{x}_4 - H_3\widetilde{x}_3 \\ J\dot{\widetilde{x}}_4 + \widetilde{W}_r^T\psi(\widehat{x}_r) + w_r &= -H_4\widetilde{x}_3 - J\kappa_r(\widetilde{x}_4 - H_3\widetilde{x}_3), \end{aligned} \tag{22}$$

where $\tilde{W}_r T = W_r^T - \widehat{W}_r^T$, $w_r = W_r^T[\psi(x_r) - \psi(\widehat{x}_r)] + \varpi_r$.

The link dynamics is the rigid dynamic model, and we take $k(x_3 - x_1)$ as the control input of the rigid dynamic model:

$$D(x_1)\dot{x}_2 + C(x_1,x_2)x_2 + G(x_1) + \mathrm{E}_l(x_1,x_2,x_3) = \tau_l. \tag{23}$$

Considerable research has been conducted on controller design for rigid robots. In this study, we opted for the widely used computed torque method with NN compensation [31] to design a controller for a rigid link. Since the link velocity is not directly measurable, we utilized the estimated velocity value instead of the actual velocity as follows:

$$\begin{aligned} \tau_l = D(x_1)[\,\ddot{q}_{ld} - K_P(x_1 - q_{ld}) - K_D(\widehat{x}_2 - \dot{q}_{ld})] \\ + C(x_1,\widehat{x}_2)\widehat{x}_2 + G(x_1) + \widehat{W}_l^T\psi(\widehat{x}_l), \end{aligned} \tag{24}$$

where K_P is the position gain matrix and K_D is the velocity gain matrix.

We choose the adaptive law of $\widehat{W}_l$ as follows:

$$\dot{\widehat{W}}_l = -F_l\psi(\widehat{x}_l)\widetilde{x}_2^T - \eta_l F_l\widehat{W}_l, \tag{25}$$

where $F_l = F_l^T$, is a positive constant matrix, $\eta_l \in \mathbf{R}$ is a positive constant.

Based on the structure of (3), we design the desired motor position vector to be:

$$x_{3d} = x_1 + k^{-1}\tau_l. \tag{26}$$

Considering the structural complexity of x_{3d}, we design the controller based DSC method for motor dynamics.

Let x_{3d} pass through a first-order filter to obtain a new variable x_{3f}:

$$\alpha_3\dot{x}_{3f} + x_{3f} = x_{3d}, x_{3f}(0) = x_{3d}(0), \tag{27}$$

where the time constant α_3 is the design constant.

Step 1: define dynamic surface error $S_3 = x_3 - x_{3f}$, whose time derivative along (27) is given by

$$\dot{S}_3 = x_4 - \left(x_{3d} - x_{3f}\right)/\alpha_3. \tag{28}$$

To stabilize S_3, a virtual control law x_{4d} is proposed as follows:

$$x_{4d} = -\eta_3 S_3 + \left(x_{3d} - x_{3f}\right)/\alpha_3, \tag{29}$$

where $\eta_3 \in R$ is a positive constant.

Let x_{4d} pass through a first-order filter to obtain a new variable x_{4f}:

$$\alpha_4 \dot{x}_{4f} + x_{4f} = x_{4d}, x_{4f}(0) = x_{4d}(0), \tag{30}$$

where the time constant α_4 is the design constant.

Step 2: define dynamic surface error $S_4 = x_4 - x_{4f}$, whose time derivative along (30) and (21) is given by:

$$\begin{aligned}\dot{S}_4 &= \widehat{x}_4 - \dot{x}_{4f} \\ &= J^{-1}\left[\tau + H_4\widetilde{x}_3 + J\kappa_r(\widetilde{x}_4 - H_3\widetilde{x}_3) + k(x_1 - x_3) - \widehat{W}_r^T\psi(\widehat{x}_3)\right] \\ &\quad -\left(x_{4d} - x_{4f}\right)/\alpha_4.\end{aligned} \tag{31}$$

A practical control law τ is proposed as follows:

$$\begin{aligned}\tau = &-k(x_1 - x_3) - H_4\widetilde{x}_3 - J\kappa_r(\widetilde{x}_4 - H_3\widetilde{x}_3) \\ &+ \widehat{W}_r^T\psi(\widehat{x}_3) + J\left[\left(x_{4d} - x_{4f}\right)/\alpha_4 - \eta_4 S_4\right],\end{aligned} \tag{32}$$

where $\eta_4 \in R$ is a positive constant.

We choose the adaptive law of $\widehat{W}_r$ as follows:

$$\dot{\widehat{W}}_r = -F_r\psi(\widehat{x}_r)\widetilde{x}_4^T - \eta_r F_r \widehat{W}_r, \tag{33}$$

where $F_r = F_r^T$, is a positive constant matrix, $\eta_r \in \mathbf{R}$ is a positive constant.

3.2. System Stability Analysis. Let

$$V = V_{ol} + V_{or} + V_{cl} + V_{cr}, \tag{34}$$

as the Lyapunov function candidate, where V_{ol} and V_{or} are, respectively, Lyapunov functions of link observer and motor observer, V_{cl} and V_{cr} are, respectively, Lyapunov functions of link controller and actuator controller.

The purpose of link controller is to make $e_1 = x_1 - q_{ld}$, $e_2 = x_2 - \dot{q}_{ld}$ converge to zero. Because x_2 cannot be measured directly, the link observer is designed to estimate x_2. If the link observer can be guaranteed to converge, and the estimated link velocity $\widehat{x}_2$ can track the expected velocity $\dot{q}_{ld}$, x_1 can track the expected position q_{ld}, it can be proved that the designed controller can guarantee the desired trajectory tracking.

Define new error variables as: $e_2 = x_2 - \dot{q}_{ld} = \widehat{x}_2 + \tilde{x}_2 - \dot{q}_{ld}$ and $e_2' = \widehat{x}_2 - \dot{q}_{ld}$, that is, as long as e_1, e_2' converges, accurate tracking can be achieved as follows:

$$\dot{e}_1 = \dot{x}_1 - \dot{q}_{ld} = x_2 - \dot{q}_{ld} = \widehat{x}_2 + \widetilde{x}_2 - \dot{q}_{ld} = e_2' + \widetilde{x}_2. \tag{35}$$

Let $e = [e_1 e_2']^T$, and substituting (24) into (16), e can be expressd as follows:

$$\dot{e} = Ae + \gamma(\widetilde{x}), \tag{36}$$

where $A = \begin{bmatrix} 0 & I \\ -K_P & -K_D \end{bmatrix}$, $\gamma(\tilde{x}) = [\kappa_l\tilde{x}_2 - (D^{-1}(x_1)H_2 - \kappa_l H_1)\tilde{x}_1]$.

Here we choose the appropriate matrix Ω to ensure that the following equation holds:

$$\Omega A + A^T\Omega = -Q, \tag{37}$$

where Q is a positive definite symmetric matrix.

Hence, we can define the following Lyapunov function of link controller:

$$V_{cl} = \frac{1}{2}e^T\Omega e. \tag{38}$$

Notice that there is an error $x_{3f} - x_{3d}$ can be expressed as follows by substituting (24) into (26):

$$\begin{aligned}r_3 &= x_{3f} - x_{3d} \\ &= x_{3f} - x_1 - k^{-1}\left[D(x_1)(\ddot{q}_{ld} - K_P(x_1 - q_{ld}) - K_D(\widehat{x}_2 - \dot{q}_{ld})) \right. \\ &\quad \left. + C(x_1, \widehat{x}_2)\widehat{x}_2 + G(x_1) + \widehat{W}_l^T\psi(\widehat{x}_l)\right].\end{aligned} \tag{39}$$

Notice that there is an error $x_{4f} - x_{4d}$ can be expressed as follows by substituting (39) into (29):

$$\begin{aligned}r_4 &= x_{4f} - x_{4d} \\ &= x_{4f} + \eta_3 S_3 - \left(x_{3d} - x_{3f}\right)/\alpha_3 = x_{4f} + \eta_3 S_3 + r_3/\alpha_3.\end{aligned} \tag{40}$$

Substituting (40) into (28), the derivative of S_3 can be expressed as follows:

$$\begin{aligned}\dot{S}_3 &= x_4 - \left(x_{3d} - x_{3f}\right)/\alpha_3 = S_4 + x_{4f} - \left(x_{3d} - x_{3f}\right)/\alpha_3 \\ &= S_4 + r_4 - \eta_3 S_3.\end{aligned} \tag{41}$$

Substituting (32) into (31), the derivative of S_4 can be expressed as follows:

$$\begin{aligned}\dot{S}_4 = \widehat{x}_4 - \dot{x}_{4f} = J^{-1}[&\tau + H_4\widetilde{x}_3 + J\kappa_r(\widetilde{x}_4 - H_3\widetilde{x}_3) \\ &+ k(x_1 - x_3) - \widehat{W}_r^T\psi(\widehat{x}_r)] \\ &-\left(x_{4d} - x_{4f}\right)/\alpha_4 = -\eta_4 S_4 + \kappa_r\widetilde{x}_4.\end{aligned} \tag{42}$$

The derivative of r_3 can be expressed as follows:

$$\dot{r}_3 = -\frac{r_3}{\alpha_3} - \Xi_3\left(e, S_3, r_3, \widehat{W}_l^T\right), \tag{43}$$

where $\Xi_3(e, S_3, r_3, \widehat{W}_l^T) = \dot{x}_1 + \left[\dot{x}_1^T \frac{\partial D}{x_1}(\ddot{q}_{ld} - K_P(x_1 - q_{ld}) - K_D(\widehat{x}_2 - \dot{q}_{ld})) + D(x_1)\left(\ddot{q}_{ld} - K_P(\dot{x}_1 - \dot{q}_{ld}) - K_D\left(\dot{\widehat{x}}_2 - \ddot{q}_{ld}\right)\right) + \dot{x}_1^T \frac{\partial G}{x_1} + \widehat{W}_1^T \dot{\psi}(\widehat{x}_l) + \left(\dot{x}_1^T \frac{\partial C}{\widehat{x}_1} + \dot{\widehat{x}}_2^T \frac{\partial C}{\widehat{x}_2}\right)\widehat{x}_2 + C(x_1, \widehat{x}_2)\dot{\widehat{x}}_2\right]$

The derivative of r_4 can be expressed as follows:

$$\dot{r}_4 = \frac{r_4}{\alpha_4} - \Xi_4\left(e, S_3, S_4, r_3, r_4, Q_{ld}, \widehat{W}_r^T\right), \tag{44}$$

where $Q_{ld} = \left[q_{ld}^T \quad \dot{q}_{ld}^T \quad \ddot{q}_{ld}^T\right]^T$, $\Xi_4(e, S_3, S_4, r_3, r_4, Q_{ld}, \widehat{W}_r^T) = -\eta_3 \dot{S}_3 - \frac{\dot{r}_3}{\alpha_3}$.

Hence, we can define the following Lyapunov function of motor controller:

$$V_{cr} = \frac{1}{2}\left[\sum_{i=3}^{4} S_i^T S_i + \sum_{i=2}^{3} r_{i+1}^T r_{i+1}\right]. \tag{45}$$

Taking the time derivative of V_{ol} and using (17) produce:

$$\begin{aligned}\dot{V}_{ol} &= \widetilde{x}_1^T \dot{\widetilde{x}}_1 + \widetilde{x}_2^T D(x_1)\dot{\widetilde{x}}_2 + \frac{1}{2}\widetilde{x}_2^T \dot{D}(x_1)\widetilde{x}_2 + tr\left(\widetilde{W}_l^T F_l^{-1}\dot{\widetilde{W}}_l\right) \\ &= \widetilde{x}_1^T(\widetilde{x}_2 - H_1\widetilde{x}_1) + \widetilde{x}_2^T\Big[C(x_1, \widehat{x}_2)\widehat{x}_2 - C(x_1, x_2)x_2 - \widetilde{W}_l^T\psi(\widehat{x}_l) - w_l \\ &\quad - D(x_1)\kappa_l\widetilde{x}_2 - (H_2 - D(x_1)\kappa_l H_1)\widetilde{x}_1\Big] + \frac{1}{2}\widetilde{x}_2^T\dot{D}(x_1)\widetilde{x}_2 + tr\left(\widetilde{W}_l^T F_l^{-1}\dot{\widetilde{W}}_l\right).\end{aligned} \tag{46}$$

Using Property 3 and (25), and considering $\dot{\widehat{W}}_l = -\dot{\widetilde{W}}_l$, (46) can be simplified as follows:

$$\begin{aligned}\dot{V}_{ol} = &-\widetilde{x}_1^T H_1\widetilde{x}_1 - \widetilde{x}_2^T[C(x_1, \widehat{x}_2) + D(x_1)\kappa_l]\widetilde{x}_2 + \widetilde{x}_2^T[I - H_2 + D(x_1)\kappa_l H_1]\widetilde{x}_1 \\ &-\widetilde{x}_2^T w_l + \eta_l tr\left(\widetilde{W}_l^T\widehat{W}_l\right).\end{aligned} \tag{47}$$

Taking the time derivative of V_{or} and using (22) produce:

$$\begin{aligned}\dot{V}_{or} = &\widetilde{x}_3^T(\widetilde{x}_4 - H_3\widetilde{x}_3) + \widetilde{x}_4^T\left(-H_4\widetilde{x}_3 - J\kappa_r\widetilde{x}_4 + J\kappa_r H_3\widetilde{x}_3 - \widetilde{W}_r^T\psi(\widehat{x}_r) - w_r\right) \\ &+ tr\left(\widetilde{W}_r^T F_r\dot{\widetilde{W}}_r\right).\end{aligned} \tag{48}$$

Using (33), and considering $\dot{\widehat{W}}_r = -\dot{\widetilde{W}}_r$, (48) can be simplified as follows:

$$\begin{aligned}\dot{V}_{or} = &-\widetilde{x}_3^T H_3\widetilde{x}_3 - \widetilde{x}_4^T J_{\kappa_r}\widetilde{x}_4 + \widetilde{x}_4^T(I - H_4 + J_r H_3)\widetilde{x}_3 \\ &-\widetilde{x}_4^T w_r + \eta_r tr\left(\widetilde{W}_r^T\widehat{W}_r\right).\end{aligned} \tag{49}$$

Taking the time derivative of V_{cl} and using (36) produce:

$$\begin{aligned}\dot{V}_{cl} &= \frac{1}{2}[\dot{e}^T\Omega e + e^T\Omega\dot{e}] \\ &= \frac{1}{2}[(Ae + \gamma(\widetilde{x}))^T\Omega e + e^T\Omega(Ae + \gamma(\widetilde{x}))] \\ &= -e^T Qe + e^T\Omega\gamma(\widetilde{x}).\end{aligned} \tag{50}$$

Taking the time derivative of V_{cr} and using (41)–(44) produce:

$$\dot{V}_{cr} = S_3^T(S_4 + r_4 - \eta_3 S_3) + S_4^T(-\eta_4 S_4 + \kappa_r \widetilde{x}_4) + \sum_{i=2}^{4} r_{i+1}^T \left(-\frac{1}{\alpha_{i+1}} r_{i+1} + \Xi_{i+1}\right). \tag{51}$$

Let $H_1 = h_1 I, H_3 = h_3 I, H_2 = I + \kappa_l h_1 D(x_1), I \in R^{3\times 3}$, $H_4 = I + \kappa_r h_3 J$.

Taking the time derivative of V and using (47)–(50) produce:

$$\begin{aligned}\dot{V} &= \dot{V}_{ol} + \dot{V}_{or} + \dot{V}_{cl} + \dot{V}_{cr} \\ &= -\widetilde{x}_1^T h_1 \widetilde{x}_1 - \widetilde{x}_2^T [C(x_1, \widehat{x}_2) + D(x_1)\kappa_l]\widetilde{x}_2 - \widetilde{x}_2^T w_l + \eta_l tr\left(\widetilde{W}_l^T \widehat{W}_l\right) \\ &- \widetilde{x}_3^T h_3 \widetilde{x}_3 - \widetilde{x}_4^T J_r \widetilde{x}_4 - \widetilde{x}_4^T w_r + \eta_r tr\left(\widetilde{W}_r^T \widehat{W}_r\right) - e^T Q e + e^T R\gamma(\widetilde{x}) + S_3^T(S_4 + r_4 - \eta_3 S_3) \\ &+ S_4^T(-\eta_4 S_4 + \kappa_r \widetilde{x}_4) + \sum_{i=2}^{3} r_{i+1}^T(-r_{i+1}/\alpha_{i+1} + \Xi_{i+1}).\end{aligned} \tag{52}$$

Then we can obtain by using Young's inequality:

$$\begin{aligned}\dot{V} \le &-h_1 \| \widetilde{x}_1\|^2 - (\kappa_l M_D - M_C) \| \widetilde{x}_2\|^2 - h_3 \| \widetilde{x}_3\|^2 - \lambda_{\min}(J\kappa_r) \| \widetilde{x}_4\|^2 \\ &- \eta_l \| \widetilde{W}_l \|_F^2 - \eta_r \| \widetilde{W}_r \|_F^2 - \lambda_{\min}(Q) \| e\|^2 - \eta_3 \| S_3\|^2 - \eta_4 \| S_4\|^2 - \frac{1}{\alpha_3} \| r_3\|^2 \\ &- \frac{1}{\alpha_4} \| r_4\|^2 + \frac{\|\widetilde{x}_2\|^2}{4} + \|w_l\|^2 + \frac{\|\widetilde{x}_4\|^2}{4} + \|w_r\|^2 + \eta_l \| \widetilde{W}_l\|_F W_{l,M} + \eta_r \| \widetilde{W}_r\|_F W_{r,M} \\ &+ \lambda_{\max}(\Omega) \| e\|^2 + \frac{\lambda_{\max}(\Omega) \| \gamma(\widetilde{x})\|^2}{4} + \frac{\|S_3\|^2}{4} + \|S_4\|^2 + \frac{\|S_3\|^2}{4} + \|r_4\|^2 \\ &+ \frac{\kappa_r \| S_4\|^2}{4} + \kappa_r \| \widetilde{x}_4\|^2 + \sum_{i=2}^{3} \left(\frac{\|r_{i+1}\|^2}{4} + \|\Xi_{i+1}\|^2\right),\end{aligned} \tag{53}$$

where $\lambda_{\min}(\cdot)$ represents the minimum eigenvalue of matrix, $\lambda_{\max}(\cdot)$ represents the maximum eigenvalue of matrix, and $W_{l,M}$ and $W_{r,M}$ are maximum eigenvalue of the weight matrix.

Using Property 1, the following inequality holds:

$$\|\gamma(\widetilde{x})\|^2 \le [\|\widetilde{x}_2\|^2 + \kappa_l \| \widetilde{x}_2\|^2 + M_{ID} \| \widetilde{x}_1\|^2], \tag{54}$$

$$\begin{aligned}\dot{V} \le &-\left(h_1 - \frac{M_{ID}\lambda_{\max}(\Omega)}{4}\right) \| \widetilde{x}_1\|^2 - \left[\kappa_l M_D - M_C - \frac{1}{4} - \frac{\lambda_{\max}(\Omega)(1+\kappa_l)}{4}\right] \| \widetilde{x}_2\|^2 \\ &-h_3 \| \widetilde{x}_3\|^2 - \left(\lambda_{\min}(J\kappa_r) - \frac{1}{4} - \kappa_r\right) \| \widetilde{x}_4\|^2 \\ &-\frac{3\eta_l}{4} \| \widetilde{W}_l \|_F^2 - \frac{3\eta_r}{4} \| \widetilde{W}_r \|_F^2 - [\lambda_{\min}(Q) - \lambda_{\max}(\Omega)] \| e\|^2 \\ &-\left(\eta_3 - \frac{1}{2}\right) \| S_3\|^2 - \left(\eta_4 - 1 - \frac{\kappa_r}{4}\right) \| S_4\|^2 - \left(\frac{1}{\alpha_3} - \frac{1}{4}\right) \| r_3\|^2 - \left(\frac{1}{\alpha_4} - \frac{1}{4}\right) \| r_4\|^2 \\ &+ \| w_l\|^2 + \|w_r\|^2 + \sum_{i=2}^{3} \| \Xi_{i+1}\|^2 + \eta_l W_{l,M}^2 + \eta_r W_{r,M}^2.\end{aligned} \tag{55}$$

Let $h_1^* = h_1 - \frac{M_{ID}\lambda_{\max}(\Omega)}{4}, h_2^* = \kappa_l M_D - M_C - \frac{1}{4} - \frac{\lambda_{\max}(\Omega)(1+\kappa_l)}{4}$, $c_l^* = \lambda_{\min}(Q) - \lambda_{\max}(\Omega), h_3^* = h_3, h_4^* = [\lambda_{\min}(J\kappa_r) - \kappa_r], \eta_3^* = (\eta_3 - \frac{1}{2}), \eta_4^* = (\eta_4 - 1 - \frac{\kappa_r}{4}), \frac{1}{\alpha_3^*} = \left(\frac{1}{\alpha_3} - \frac{1}{4}\right), \frac{1}{\alpha_4^*} = \left(\frac{1}{\alpha_4} - \frac{1}{4}\right)$, and they are all positive, and it follows that:

$$\begin{aligned} \dot{V} \leq & -\sum_{i=1}^{4} h_i^* \parallel \widetilde{x}_i \parallel^2 - c_l^* \\ & \parallel e \parallel^2 - \sum_{i=3}^{4} \eta_i^* \parallel S_i \parallel^2 - \sum_{i=2}^{3} \frac{\parallel r_i \parallel^2}{\alpha_{i+1}^*} - \frac{3\eta_l}{4} \parallel \widetilde{W}_l \parallel_F^2 - \frac{3\eta_r}{4} \parallel \widetilde{W}_r \parallel_F^2 \\ & + \parallel w_l \parallel^2 + \parallel w_r \parallel^2 + \sum_{i=2}^{3} \parallel \Xi_{i+1} \parallel^2 + \eta_l W_{l,M}^2 + \eta_r W_{r,M}^2 \leq -2\rho V + \Upsilon, \end{aligned} \tag{56}$$

where $\rho \in [0, \min(h_1^*, \frac{h_2^*}{M_D}, h_3^*, \frac{h_4^*}{M_J}, \eta_3^*, \eta_4^*, \frac{1}{\alpha_3^*}, \frac{1}{\alpha_4^*}, \frac{c_1^*}{\lambda_{\max}(\Omega)}, \frac{3\eta_l\lambda_{\min}(F_l)}{4}, \frac{3\eta_r\lambda_{\min}(F_r)}{4})]$ and $\Upsilon = \|w_l\|^2 + \|w_r\|^2 + \sum_{i=2}^{3} \parallel \Xi_{i+1} \parallel^2 + \eta_l W_{l,M}^2 + \eta_r W_{r,M}^2$.

By selecting the appropriate parameters, we can make $\rho \geq \Upsilon/2\mu$, when $V(t) = \mu$, $\dot{V} \leq 0$, $V(t) \leq \mu$ is an invariant set. Therefore,

$$0 \leq V \leq \Upsilon/2\rho + [V(0) - \Upsilon]/(2\rho e^{-2\rho t}). \tag{57}$$

The inequality (57) illustrates the results that the system tracking errors, velocity observation errors, and NNs weights estimation errors will converge to a ball with a small radius determined by Υ and ρ, and then all the system states are SGUUB.

4. Simulation Results

This section shows a comparison study between our proposed scheme and the standard DSC method, to demonstrate the main contribution of our proposed control scheme.

To evaluate the dynamic behavior of the proposed control scheme, consider the single-link robotic manipulator with flexible joint [32]. The dynamic model is given by:

$$\begin{aligned} D\,\ddot{q}_l + \text{mglsin}(q_l) + k(q_l - q_r) &= \tau_{dl} \\ J\,\ddot{q}_r - k(q_l - q_r) &= \tau + \tau_{dr}. \end{aligned} \tag{58}$$

The nominal parameters are $m = 2\,kg, l = 1\,m$, $k = 10\,N \cdot m/\text{rad}$, $D = 2\,kg \cdot m^2$, and $J = 0.5\,kg \cdot m^2$. The initial states are set as $[q_l(0), \dot{q}_l(0), q_r(0), \dot{q}_r(0)]^T = [0, 0, 0, 0]^T$. The parameters of link observer are set as $H_1 = 200, \kappa_l = 10, h_1 = 200, H_2 = I + \kappa_l h_1 D(x_1)$. The parameters of motor observer are set as $H_3 = 200, \kappa_r = 50, h_3 = 200, H_4 = I + \kappa_r h_3 J$. The parameters of DSC controller are set as $\alpha_3 = 0.001, \alpha_4 = 0.001, \eta_3 = 100, \eta_4 = 200$. The parameters of adaptive law (25) are set as $F_l = 1200, \eta_l = 0.0001$. The parameters of adaptive law (33) are set as $F_r = 0.00001, \eta_r = 0.0001$.

First, suppose that the dynamic model of RMFJ adopts the nominal parameters and the link velocity is not available, the proposed control scheme is used for the tracking control of the RMFJ and the desired trajectory is given by $q_{ld} = \sin(t)$. Besides the proposed control scheme, the comparative studies are performed by using the standard DSC controller, the parameters of the standard DSC controller are set as $\alpha_2 = 0.01, \alpha_3 = 0.01, \alpha_4 = 0.01, \eta_1 = 5, \eta_2 = 45, \eta_3 = 25, \eta_4 = 5$, and the link velocity is available.

It is noting that if the input torque τ is directly used, it will lead to algebraic loop problems. The method we adopt is to pass τ through a low-pass filter to obtain τ_f. Because the actuator has low-frequency characteristics, τ_f is approximately equal to τ in the low-frequency range. Therefore, in the simulation, we use τ_f instead of τ.

The simulation results are shown in Figures 2–4. Figure 2 displays the system output trajectories ($q_l(P)$ and $q_l(D)$) of the proposed and standard DSC method, and the given reference signal q_{ld}. We can see that the proposed control scheme and the DSC controller both achieve satisfactory control performance from Figure 2. Figure 3 shows the curves of tracking errors of both methods. Figure 4 shows that the error of the link observer. These results show that all the variables in the closed-loop system are bounded.

Figure 3 is a good illustration of the effectiveness of our proposed control scheme, where we choose the performance measure of maximum tracking error to compare the tracking performance of the system. The maximum tracking errors of these two methods in steady state are 0.0018 and 0.0191, respectively. It is shown that the tracking errors converge to a small neighborhood around the origin, and the tracking error of the proposed control scheme is smaller than that of the DSC controller. To further compare the tracking performance of the two control schemes, the ITAE index is calculated. The ITAE index of the proposed control scheme is 0.0093, and the ITAE index of the standard DSC method is 0.4513. It follows that the tracking performance of the proposed control scheme is better.

Remark 4. It is worth noting that the DSC method does not consider the errors caused by the introducing of first-order filters. In order to achieve precise control performance, in our proposed control scheme, the DSC acts only on motor dynamics, reducing the error accumulation caused by first-order filters. The simulation results, especially those in Figure 3, demonstrate the main contribution of our proposed control scheme.

Next, in order to illustrate the robustness of the control method, we made a change of 10% in the model nominal parameters. The actual model parameters and the external

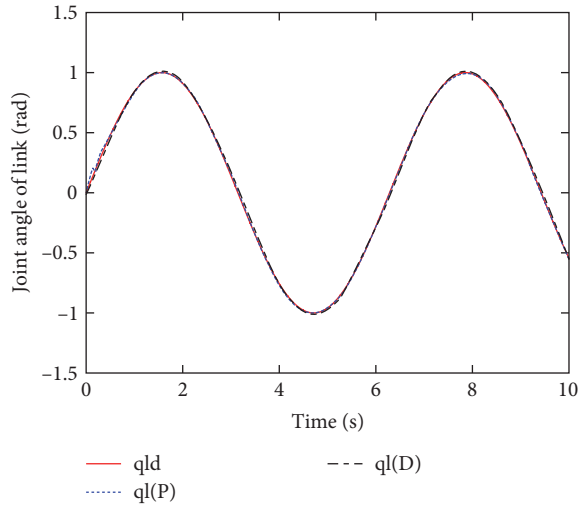

Figure 2: The system output of q_l of the proposed and DSC method.

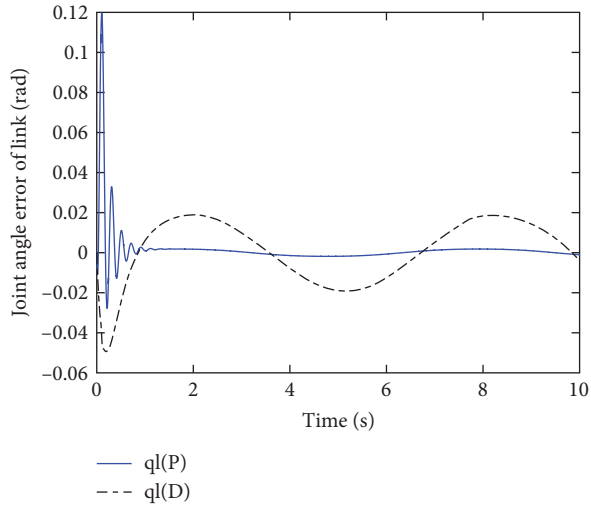

Figure 3: The joint errors of the proposed and DSC method.

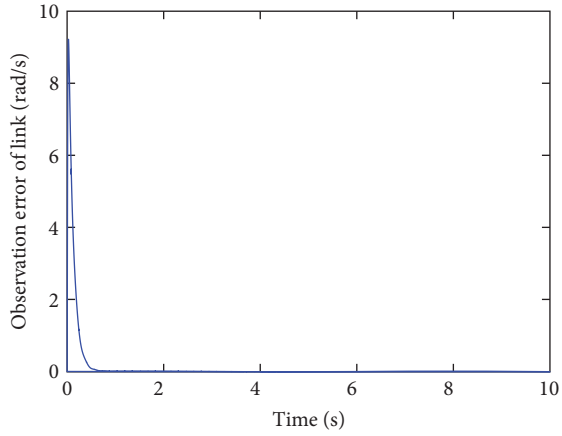

Figure 4: The error of the link state observer.

disturbances are set as $\widehat{m} = 1.1\,m$, $\widehat{l} = 1.1\,l$, $\widehat{D} = 1.1\,D$, $\widehat{k} = 1.1\,k$, $\widehat{J} = 1.1\,J$, $\tau_{dl} = 50\sin(8t)$, and $\tau_{dr} = 100\sin(8t)$. The simulation results are shown in Figures 5–8. Figure 5

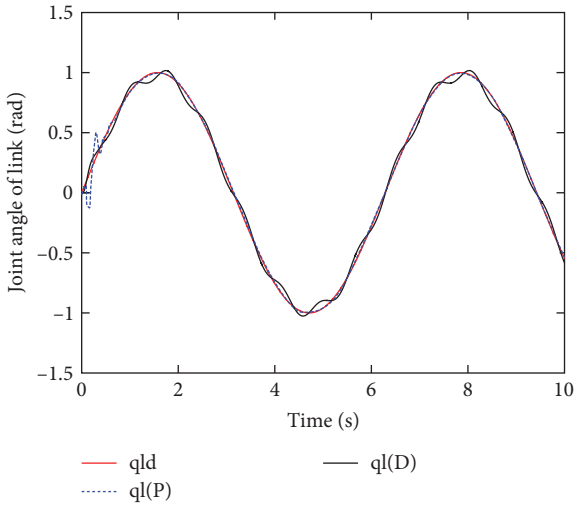

Figure 5: The system output of q_l of the proposed and DSC method.

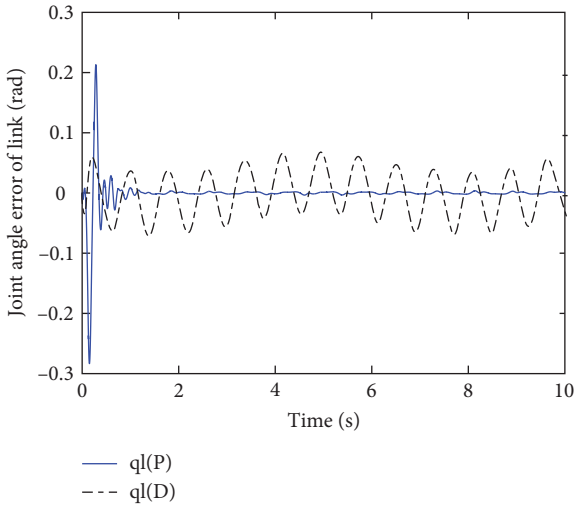

Figure 6: The joint errors of the proposed and DSC method.

displays the system output trajectories ($q_l(P)$ and $q_l(D)$) of the proposed and the standard DSC method, and the given reference signal q_{ld}. In Figure 5, the link position of the DSC controller shows an obvious vibration under the influence of parameter uncertainty and external disturbances. It can be observed from Figures 5–7 that even if the estimated parameters have large deviations and RMFJ is subjected to large external disturbance, the state observers can still accurately estimate the velocities of the link and the motor. The proposed control scheme in this paper can effectively achieve accurate trajectory tracking of link and suppress vibration of the flexible joints. The simulation results show that the proposed control scheme is robustness to external disturbance and the parameter uncertainty.

5. Conclusions

This paper proposed a novel control scheme for RMFJ. The issue associated with the tracking control of the RMFJ in the

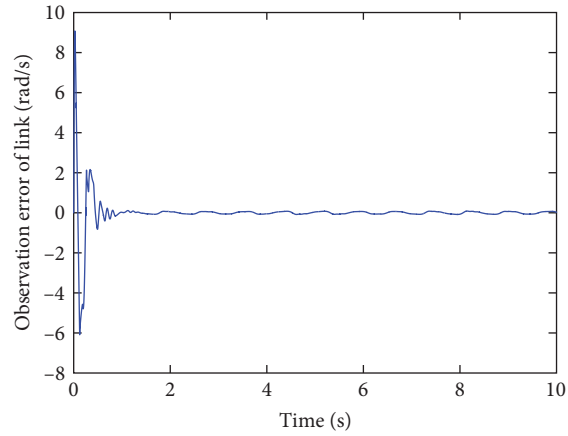

Figure 7: The error of the link state observer.

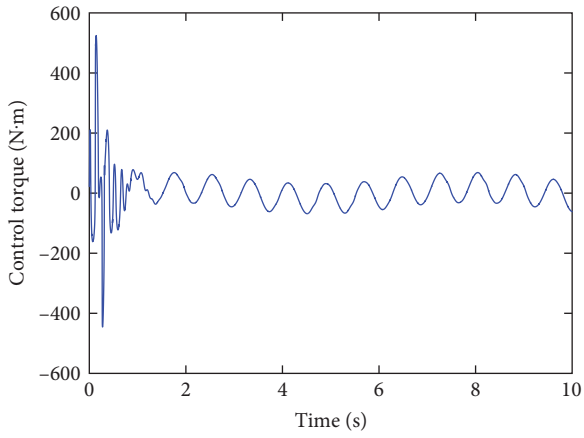

Figure 8: System control torque.

presence of system uncertainties and external disturbances is solved. Meantime, the proposed control scheme does not require link velocity measurements and high-order derivatives of the link states. The control scheme employs the NNs-based observers to estimate both motor velocity and link velocity. By using the virtually applied torque, the link controller is designed based on rigid link dynamics and the motor controller is designed by using DSC technique. The semiglobally uniformly ultimate boundedness of all signals within the closed-loop system is guaranteed by using the Lyapunov method. Numerical simulation results show that system output tracking errors converge to a small neighborhood around the origin. The standard DSC method is compared with the proposed control scheme, showing that the proposed control scheme can get better performance.

Data Availability

The data used to support the findings of this study are available from the corresponding author upon request.

Conflicts of Interest

The author declares that there is no conflicts of interest.

References

[1] Y. Zhang, L. Cheng, R. Cao, H. Li, and C. Yang, "A neural network based framework for variable impedance skills learning from demonstrations," *Robotics and Autonomous Systems*, vol. 160, Article ID 104312, 2023.

[2] P. Jia, "Control of flexible joint robot based on motor state feedback and dynamic surface approach," *Journal of Control Science and Engineering*, vol. 2019, Article ID 5431636, 12 pages, 2019.

[3] P. Zhao and Y. Zhou, "Active vibration control of flexible-joint manipulators using accelerometers," *Industrial Robot*, vol. 47, no. 1, pp. 33–44, 2019.

[4] B. Rahmani and M. Belkheiri, "Adaptive neural network output feedback control for flexible multi-link robotic manipulators," *International Journal of Control*, vol. 92, no. 10, pp. 2324–2338, 2019.

[5] A. De Luca, B. Siciliano, and L. Zollo, "PD control with on-line gravity compensation for robots with elastic joints: theory and experiments," *Automatica*, vol. 41, no. 10, pp. 1809–1819, 2005.

[6] Z.-Y. Chen and L. Chen, "Study on dynamics modeling and singular perturbation control of free-floating space robot with flexible joints," *China Mechanical Engineering*, vol. 22, no. 18, pp. 2151–2155, 2011.

[7] C. Y. Yang, Y. M. Xu, and W. Dai, "Two-time-scale composite control of flexible manipulators," *Control Theory & Applications*, vol. 36, no. 4, pp. 158–164, 2019.

[8] J.-W. Huang and J.-S. Lin, "Backstepping control design of a single-link flexible robotic manipulator," *IFAC Proceedings Volumes*, vol. 41, no. 2, pp. 11775–11780, 2008.

[9] F. Petit, A. Daasch, and A. Albu-Schäffer, "Backstepping control of variable stiffness robots," *IEEE Transactions on Control Systems Technology*, vol. 23, no. 6, pp. 2195–2202, 2015.

[10] J. H. Oh and J. S. Lee, "Control of flexible joint robot system by backstepping design approach," *Intelligent Automation & Soft Computing*, vol. 5, no. 4, pp. 267–278, 1999.

[11] F. Ghorbel, J. Y. Hung, and M. W. Spong, "Adaptive control of flexible-joint manipulators," *IEEE Control Systems Magazine*, vol. 9, no. 7, pp. 9–13, 1989.

[12] M.-C. Chien and A.-C. Huang, "Adaptive control for flexible-joint electrically driven robot with time-varying uncertainties," *IEEE Transactions on Industrial Electronics*, vol. 54, no. 2, pp. 1032–1038, 2007.

[13] H. Sira-Ramirez and M. W. Spong, "Variable structure control of flexible joint manipulators," *International Journal of Robotics and Automation*, vol. 3, no. 2, pp. 57–64, 1988.

[14] A.-C. Huang and Y.-C. Chen, "Adaptive sliding control for single-link flexible-joint robot with mismatched uncertainties," *IEEE Transactions on Control Systems Technology*, vol. 12, no. 5, pp. 770–775, 2004.

[15] W. He, Z. Yan, Y. Sun, Y. Ou, and C. Sun, "Neural-learning-based control for a constrained robotic manipulator with flexible joints," *IEEE Transactions on Neural Networks and Learning Systems*, vol. 29, no. 12, pp. 5993–6003, 2018.

[16] Y. Yang, T. Dai, C. Hua, and J. Li, "Composite NNs learning full-state tracking control for robotic manipulator with joints flexibility," *Neurocomputing*, vol. 409, pp. 296–305, 2020.

[17] W. Sun, S.-F. Su, J. Xia, and V.-T. Nguyen, "Adaptive fuzzy tracking control of flexible-joint robots with full-state constraints," *IEEE Transactions on Systems, Man, and Cybernetics: Systems*, vol. 49, no. 11, pp. 2201–2209, 2018.

[18] H. Shi, M. Wang, and C. Wang, "Pattern-based autonomous smooth switching control for constrained flexible joint manipulator," *Neurocomputing*, vol. 492, pp. 162–173, 2022.

[19] X. Liu, C. Yang, Z. Chen, M. Wang, and C.-Y. Su, "Neuro-adaptive observer based control of flexible joint robot," *Neurocomputing*, vol. 275, pp. 73–82, 2018.

[20] L. Cao, Y. Pan, H. Liang, and T. Huang, "Observer-based dynamic event-triggered control for multiagent systems with time-varying delay," *IEEE Transactions on Cybernetics*, vol. 53, no. 5, pp. 3376–3387, 2023.

[21] D. Swaroop, J. K. Hedrick, P. P. Yip, and J. C. Gerdes, "Dynamic surface control for a class of nonlinear systems," *IEEE Transactions on Automatic Control*, vol. 45, no. 10, pp. 1893–1899, 2000.

[22] S. J. Yoo, J. B. Park, and Y. H. Choi, "Adaptive dynamic surface control of flexible-joint robots using self-recurrent wavelet neural networks," *IEEE Transactions on Systems, Man and Cybernetics, Part B (Cybernetics)*, vol. 36, no. 6, pp. 1342–1355, 2006.

[23] L. Cao, Z. Cheng, Y. Liu, and H. Li, "Event-based adaptive NN fixed-time cooperative formation for multiagent systems," *IEEE Transactions on Neural Networks and Learning Systems*, 2022.

[24] S. Ling, H. Wang, and P. X. Liu, "Adaptive tracking control of high-order nonlinear systems under asymmetric output constraint," *Automatica*, vol. 122, Article ID 109281, 2020.

[25] J. A. Farrell, M. Polycarpou, M. Sharma, and Wenjie Dong, "Command filtered backstepping," *IEEE Transactions on Automatic Control*, vol. 54, no. 6, pp. 1391–1395, 2009.

[26] S. Ling, H. Wang, and P. X. Liu, "Adaptive fuzzy tracking control of flexible-joint robots based on command filtering," *IEEE Transactions on Industrial Electronics*, vol. 67, no. 5, pp. 4046–4055, 2019.

[27] H. Liang, L. Chen, Y. Pan, and H.-K. Lam, "Fuzzy-based robust precision consensus tracking for uncertain networked systems with cooperative–antagonistic interactions," *IEEE Transactions on Fuzzy Systems*, vol. 31, no. 4, pp. 1362–1376, 2023.

[28] S. Ling, H. Wang, and P. X. Liu, "Adaptive fuzzy dynamic surface control of flexible-joint robot systems with input saturation," *IEEE/CAA Journal of Automatica Sinica*, vol. 6, no. 1, pp. 97–107, 2019.

[29] Y.-C. Chang and H.-M. Yen, "Design of a robust position feedback tracking controller for flexible-joint robots," *IET Control Theory & Applications*, vol. 5, no. 2, pp. 351–363, 2011.

[30] S. S. Ge, C. C. Hang, T. H. Lee, and T. Zhang, *Stable Adaptive Neural Network Control*, vol. 13 of The International Series on Asian Studies in Computer and Information Science, Springer Science & Business Media, 2013.

[31] G. Feng, "A compensating scheme for robot tracking based on neural networks," *Robotics and Autonomous Systems*, vol. 15, no. 3, pp. 199–206, 1995.

[32] M. W. Spong, "Adaptive control of flexible joint manipulators," *Systems & Control Letters*, vol. 13, no. 1, pp. 15–21, 1989.